ISSN 1068-3755, Surface Engineering and Applied Electrochemistry, 2020, Vol. 56, No. 4, pp. 474–483. © Allerton Press, Inc., 2020.

Characteristics and Parameters of Overstressed Nanosecond-Pulse Discharge Plasma between Chalcopyrite ($CuInSe_2$) Electrodes in Argon

A. K. Shuaibov[a, *], A. Y. Minya[a], Z. T. Gomoki[a], R. V. Hrytsak[a], A. A. Malinina[a], A. N. Malinin[a], V. M. Krasilinets[b], and A. M. Solomon[b]

[a] *Department of Quantum Electronics, Uzhgorod National University, Uzhgorod, 88000 Ukraine*
[b] *Institute of Electron Physics, National Academy of Sciences of Ukraine, Uzhhorod, 88017 Ukraine*
**e-mail: alexsander.shuaibov@uzhnu.edu.ua*

Received October 30, 2019; revised December 4, 2019; accepted December 4, 2019

Abstract—A bipolar nanosecond discharge with a voltage amplitude of one polarity of 15–40 kV and a current amplitude of 50–150 A in a pulse was ignited at an inter-electrode distance of 0.1 cm and the pressure of argon 101 or 202 kPa, at a frequency of the pulse voltage 40–100 Hz. The pulsed electric discharge power was in a range of 5–11 MW, with a plasma energy input of 0.40 and 0.44 J per pulse. Spectroscopic plasma diagnostics showed that the spectral lines of the copper atom in the range 200–230 nm and the spectral lines of the indium atom and Cu^+ and In^+ ions in a longer wavelength range of the spectrum are the most intense. The following lines from the spectral range of 300–460 nm can be used to diagnose the deposition of chalcopyrite films in real time: 307.38 nm Cu(I), 329.05 nm Cu(I), 410.17 nm In(I), 451.13 nm In(I). By solving the Boltzmann kinetic equation for the electron energy distribution function, the temperature and the density of electrons, the specific losses of the discharge power on the main electronic processes and the rate constants of the electronic processes depending on the value of the parameter of the ratio of the electric field strength E to the total concentration of Ar atoms and a small admixture of a Cu vapor N (E/N) are simulated. In a discharge in a mixture of copper vapor with argon, the electron temperature increased in a range of 300–110000 K, with a change in the E/N parameter from 1 to 1800 Td. The electron concentration was in a range of $2.1 \times 10^{20} - 2.7 \times 10^{20}$ m^{-3}, at a current density $(612–765) \times 10^6$ A/m^2 on the electrode surface (at $E/N = 1676$ Td). Thin films of chalcopyrite were synthesized on substrates of transparent solid dielectrics, which, in a wide spectral range of 200–800 nm, absorb radiation incident of their surface quite effectively. This opens up prospects for their use in photovoltaic devices. It was shown that the smallest transmission of radiation is characteristic of chalcopyrite films synthesized at atmospheric pressure of argon and air.

Keywords: overstressed nanosecond discharge, atmospheric pressure plasma, chalcopyrite, argon, thin films
DOI: 10.3103/S1068375520040158

INTRODUCTION

It is known that chalcopyrite films of the $CuInSe_2$ type find wide practical applications in photovoltaic devices, including solar batteries [1]. Among the physical methods of chalcopyrite film synthesis, there is a well-known method of laser deposition of films. This method preserves the stoichiometric composition of the film relative to a massive target. However, it is an expensive method and has technological difficulties in the synthesis of large area films. In [2], the results of the study of the charac-teristics and parameters of a plasma of an overstressed nanosecond discharge based on vapors of $CuInSe_2$ and $CuSbSe_2$ compounds and atmospheric air are presented. Besides, the sputtering of chalcopyrite electrodes was carried out in a strong electric field of an overstressed nanosecond discharge, where the formation of ectons plays a significant role [3].

The presence of oxygen in the plasma of such a discharge between copper electrodes leads to the formation of copper oxide nanostructures [4]. When sputtering electrodes in the air, the effect of oxygen on deposited chalcopyrite films, from the point of view of applications in photovoltaic devices, can be negative. Therefore, it is relevant to study the sputtering of chalcopyrite electrodes in strong electric fields using oxygen-free gas media. The investigations of the characteristics and parameters of such plasma in close relationship with the characteristics of the synthesized chalcopyrite films is also important.

This paper presents the results of studying the electrical and optical characteristics, as well as the parameters, of the overstressed nanosecond discharge plasma between electrodes based on $CuInSe_2$ in argon, at atmospheric pressure.

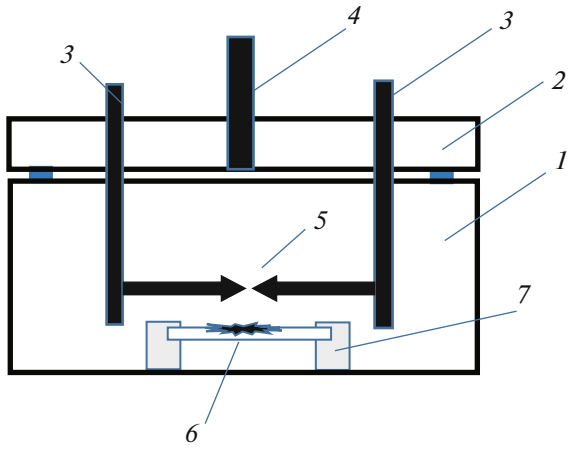

Fig. 1. Scheme of discharge device for the synthesis of chalcopyrite thin films on glass or quartz surfaces of: (*1*) plexiglas discharge chamber; (*2*) upper flange; (*3*) hermetic metal leads; (*4*) fitting for connecting to a vacuum gas mixing system; (*5*) electrodes with chalcopyrite; (*6*) glass substrate with a film based on sputtered electrodes; and (*7*) plate fixing system.

EXPERIMENTAL

Electrodes based on $CuInSe_2$ were installed in a sealed dielectric chamber (Fig. 1). The interelectrode distance in the experiments was 1 mm; therefore, the nanosecond discharge was vastly overstressed. The discharge chamber was preliminarily pumped out to a residual air pressure of 10 Pa and then filled with high-purity argon to pressures of 101 or 202 kPa. To reduce the influence of electromagnetic interference on the system for recording characte-ristics of a nanosecond discharge, a camera with an electrode system was installed in a screen made of a metal mesh. The diameter of the chalcopyrite cylindrical electrodes was 5 mm, and the radius of curvature of their working end part was 3 mm.

To ignite the discharge, bipolar nanosecond voltage pulses with amplitudes of positive and negative polarity in a range of 15–40 kV were applied to the electrodes. The voltage and current pulses had a total duration of 50–150 ns. The amplitude of the current pulses was in a range of 50–150 A. The pulse repetition rate of the modulator was in a range of 40–1000 Hz, but the main studies were carried out at a frequency of 100 Hz. The voltage pulses at the discharge gap and the discharge current were measured using a wide-band capacitive divider, a Rogowski coil, and a 6-LOR-04 wide-band oscilloscope. The time resolution of this registration system was 2–3 ns. To record the plasma emission spectra, an MDR-2 monochromator, an FEU-106 photomultiplier, a DC amplifier, and a computer-based automated spectra registration system were used. The radiation of the discharge plasma was analysed in a spectral range of 200–650 nm. The plasma radiation detection system was calibrated using a deuterium lamp radiation in a spectral range of 200–400 nm and a gang-lamp in the wavelength range of 400–650 nm.

When burning a nanosecond discharge in a repetitively pulsed mode (f = 40–100 Hz) for 2–3 h on a dielectric substrate, set at a distance of 3 cm from the center of the discharge gap, a gray film was deposited from the sputtered products of the electrode material. The obtained samples of chalcopyrite-based films were investigated for light transmission in a wide wavelength range (200–850 nm) in order to establish the prospects of their use in photovoltaic devices.

Other experimental conditions for studying the characteristics of a nanosecond discharge were the same as in [2, 4], where the results of a study of the characteristics of the same discharge in atmospheric air between the electrodes based on $CuIn(Sb)Se_2$ compounds are presented.

The transmission spectra of chalcopyrite films were studied using a spectral complex based on an MDR-23 monochromator, at room temperature, in the 200–850 nm wavelength range [5, 6]. The optical scheme of the complex is shown in Fig. 2.

The radiation source (*3*) allows to conveniently change a heat lamp with a heated tungsten electrode to a DDS-30 gas-discharge deuterium lamp when switching the transmission spectra from the visible to the UV region. The radiation from the lamps was collected by a quartz condenser (*4*) and focused on the entrance slit of the MDR-23 monochromator (*6*). Subsequently, monochromatic radiation fell on the sample under study (*1*), which was mounted on the holder of the measuring chamber (*2*). The intensity of the radiation transmitted by the sample is measured by a photomultiplier (PMT-100) (*7*) using a recording

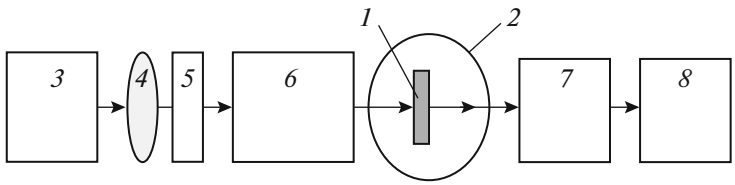

Fig. 2. Optical installation system to study transmission spectra of films: (*1*) sample; (*2*) measuring chamber; (*3*) combined light source; (*4*) condenser; (*5*) light filters; (*6*) MDR-23 monochromator; (*7*) photomultiplier tube; and (*8*) radiation detection system.

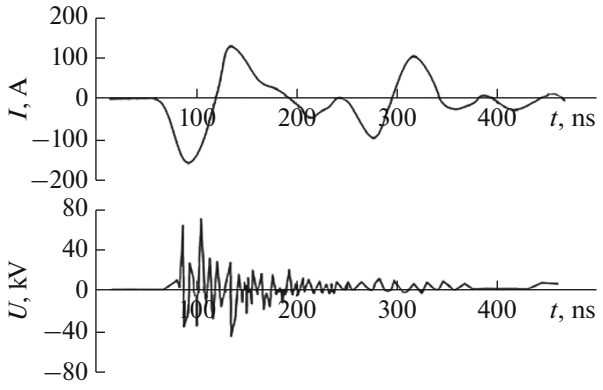

Fig. 3. Oscillograms of current and voltage between chalcopyrite electrodes at Ar pressure of 101 kPa.

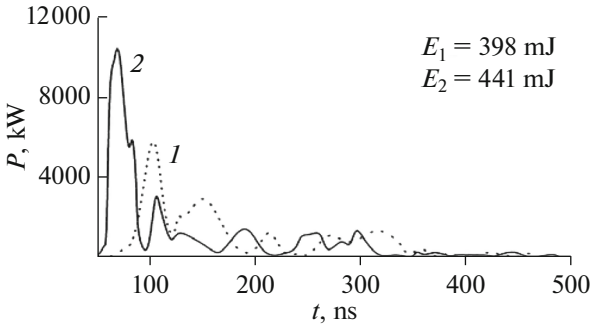

Fig. 4. Pulsed power of overstressed nanosecond discharge: f = 100 Hz; distance between electrodes with $CuInSe_2$ of 1 mm; and argon pressures: (*1*) p(Ar) = 101 kPa; and (*2*) p(Ar) = 202 kPa.

system (*8*). The registration of the experimental data from the photomultiplier output was provided via a special program that specified the required number of photon counts at each point of a given spectral range and the step of scanning the transmission spectrum, as well as the initial and final wavelengths. This program allows controlling the stepper motor of the MDR-23 monochromator.

ELECTRICAL AND OPTICAL CHARACTERISTICS

An overstressed nanosecond discharge between chalcopyrite electrodes in argon (Ar) (p = 101; 202 kPa) had a diffuse character, although it was ignited in a rather non-uniform electric field without using a separate preionization system. This is possible if the role of the preionization system is performed by X-rays from plasma of similar discharges or in the presence of a runaway electron beam [7, 8].

The characteristic oscillograms of voltage pulses at the discharge gap and the discharge current are shown in Fig. 3. They were similar to those given in [2, 4] for the same discharge between chalcopyrite electrodes at atmospheric air pressure. The electric pulsed power of an overstressed nanosecond discharge is shown in Figure 4 with p(Ar) = 101 and 202 kPa. In the experiment, voltage oscillations were observed across the gap with a half-period of ~10 ns, which are caused by the mismatch of the output impedance of the high-voltage pulse generator with the load. With an Ar pressure of 101 kPa, the maximum amplitude of the voltage surges reached 40–60 kV, and with an increase in the Ar pressure to 202 kPa and, accordingly, the increase in the resistance of the discharge medium, the voltage amplitude increased to 60–70 kV.

The current pulses had the form of current oscillations damping with time, with the duration of an individual maximum at a level of 50–70 ns with the total duration of the current pulse train of 400–500 ns. The amplitude of the current surges was 150–120 A (p = 101 kPa) and 180–120 A (p = 202 kPa). The current pulses were partially integrated over time by the Rogowski coil, so the voltage and current oscillograms differed from each other.

The main part of the electric power was introduced in the discharge in the first 150–200 ns. The maximum value of the pulsed electrical power introduced in plasma reached ~5–6 MW at p = 101 kPa and 10.05 MW at p = 202 kPa. In the time interval t = 150–300 ns, the discharge was maintained by pulsed power oscillations at a level of ~ 0.15 MW. The energy input in the pulse for a discharge at an Ar pressure of 101 kPa was about 400 and 440 mJ at p = 202 kPa.

Such a character of the pulsed energy deposition, which is implemented in the mode of the mismatch of the output impedance of the generator of high voltage nanosecond voltage pulses with the resistance of the discharge plasma, contributes to the effective sputtering of the electrode material and its deposition on a solid dielectric substrate [9, 10].

As demonstrated in Fig. 4, with an increase in the Ar pressure, the matching of the output resistance of the high-voltage modulator with the resistance of the discharge plasma improves, and the energy input per discharge pulse increases from 398 to 441 mJ.

Figure 5 shows the plasma emission spectrum of an overstressed nanosecond discharge between electrodes from $CuInSe_2$ at p(Ar) = 101 kPa. With an increase in the Ar pressure to 202 kPa, the character of the spectrum did not change significantly, only the radiation intensities of individual spectral lines changed. Table 1 presents the results of the interpretation of the most intense spectral lines in the plasma emission spectra with p(Ar) = 101 and 202 kPa (spectral lines 1–15).

The emission spectrum of the discharge plasma consisted of a group of intense spectral lines predominantly of a copper atom and a single-charged indium ion In^+ in the spectral range 200–230 nm, as well as for plasma produced in an overstressed nanosecond

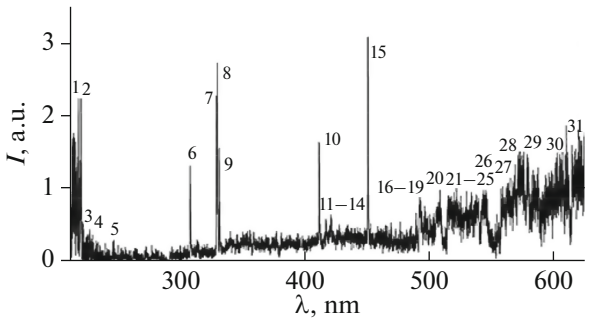

Fig. 5. Plasma emission spectrum of overstressed nanosecond discharge between chalcopyrite electrodes with $p(Ar) = 101$ kPa.

discharge between copper electrodes in atmospheric air at an interelectrode distance of $d = 2$ mm [11–13] (in terms of copper atoms). This group of spectral lines has not been previously studied when sputtering electrodes from $CuInSe_2$ in atmospheric air ($d = 2$ mm) in this type of discharge [2]. An increase in the Ar pressure to 202 kPa led to a decrease in the intensity of the spectral lines 218.17 and 219.95 nm of the Cu atom, which is probably due to an increase in the absorption of UV radiation and an increase in the vapor density of chalcopyrite or its destruction products in the discharge, as this increases the pulsed energy contribution to plasma. In addition, the spectral line 218.17 nm Cu(I) had a lower ground energy level of Cu(I) and is characterized by self-absorption in the Cu vapor. The intensities of the indium ion In^+ spectral lines with increasing argon pressure and the energy deposition in the plasma increased (Table 1), as well as the intensities of the copper ion Cu^+ lines for the discharge between Cu electrodes in atmospheric pressure [11, 12].

In the study of UV radiation of a high-voltage multielectrode discharge in atmospheric air, in which a high-current nanosecond discharge was successively ignited in six discharge gaps of 1.5 mm each, and using Cu electrodes, close plasma spectral characteristics were obtained in the 200–250 nm wavelength range [14].

The second group of spectral lines (Table 1, lines 6–15) was observed against the background of continuous radiation of low intensity, but the intensity slightly increased with increasing wavelength (Fig. 5). The intensities of these spectral lines of copper and indium atoms, as well as singly charged argon ions Ar^+, increased at a higher Ar pressure, the pulsed energy input to plasma, and hence the density of the chalcopyrite vapor or its decay products in the discharge.

The radiation in the spectral range 460–630 nm had the form of molecular bands; against the their background, individual low-intensity spectral lines of atoms or ions were also recorded. It is likely that the emission spectrum of the discharge in this wavelength range is due to the emission of selenium molecules, as well as atoms and argon ions. Accurate identification of this part of the spectrum requires the use of a spectrophotometer with a higher spectral resolution.

To diagnose the deposition of chalcopyrite films on solid glass or quartz substrates in real time, it is possible to use intense spectral lines of Cu and In atoms separately located in the wavelength range 300–460 nm: 307.38 nm Cu(I), 329.05 nm Cu(I), 410.17 nm In(I), 451.13 nm In(I).

NUMERICAL SIMULATION OF PLASMA PARAMETERS

Estimated calculations of some plasma parameters were carried out for a low average copper vapor density (approximately 30 Pa), characteristic for the working medium of low-pressure ion discharge gas lasers on transition metal vapors [15]. The data of [16] were also taken into account, where the results of the study of atmospheric pressure air plasma with a small admixture of copper vapor are also approximately at a level of 30 Pa, which entered the plasma as a result of the erosion of copper electrodes.

To the best of the authors' knowledge, so far there is no information on the following: at atmospheric Ar pressures 101 and 202 kPa, the leading edge of the voltage pulse (5–7 ns) has a relatively long duration of as well as on the data on the threshold values of the ratio of the electric field strength E to the total concentration of Argon atoms and a small admixture of a Cu vapor (E/N) when the runaway of electrons becomes essential for the system of electrodes with a weak nonuniform distribution of the electric field strength in the discharge gap. Under such experimental conditions, the most likely factor in the pre-ionization of the interelectrode gap is X-ray radiation [17]. In the present experimental work, small average partial pressures of Cu vapors over the discharge region were indicated by a small pulse repetition rate (40–100 Hz) and small autographs on the working surface of the electrodes. As in [18], traces of erosion had the form of individual points with diameters up to 100–200 μm, which relatively uniformly filled the working surface of the electrodes. Under the experimental conditions of the present work, the maximum value of the parameter E/N reached at $p(Ar) = 101$ kPa and $d = 1$ mm was approximately 1700 Td, which is less than the critical value E/N for nitrogen, according to the local electron runaway criterion—1787.7 Td [19, 20]. The latest results of numerical simulation of the runaway electron generation in nitrogen at atmospheric pressure in the needle–plane electrode system showed that this threshold is even higher and amounts to 4000 V/(cm Torr) [21].

Therefore, for the estimated calculations of the parameters of atmospheric pressure plasma with small additions of the decomposition products of chalcopyrite molecules, the Bolsig + software, version 12/2017, a standard program for solving the Boltzmann kinetic

Table 1. Results of identification of most intense spectral lines of products of destruction of chalcopyrite in overstressed nanosecond discharge, at Ar pressure 101 and 202 kPa

No.	λ, nm	I, a.u. (at p(Ar) = 101 kPa)	I, a.u. (at p(Ar) = 202 kPa)	Object	E_{low}, eV	E_{up}, eV	Lower level	Upper level
1	218.172	2.26	0.33	Cu(I)	0.00	5.68	$4s\,^2S$	$4p'\,^2P^0$
2	219.95	2.26	0.37	Cu(I)	1.39	7.02	$4s^2\,^2D$	$4p''\,^2D^0$
3	225.57	0.34	1.66	In(II)	12.68	18.17	$5s5d\,^3D_3$	$5s4f\,^3F^0$
4	226.37	0.4	1.64	Cu(II)	8.92	14.39	$4p'\,^1F^0$	$4d\,^3G$
5	246.018	0.3	0.41	In(II)	12.68	17.72	$5s5d\,3D$	$5s7f\,^3F^0$
6	307.379	1.32	1.70	Cu(I)	1.39	5.42	$4s^2\,^2D$	$4p'\,2F^0$
7	328.27	2.13	2.35	Cu(I)	5.15	8.93	$4p'\,^4F^0$	$4d'\,^2G$
8	329.05	2.74	3.27	Cu(I)	5.07	8.84	$4p'\,^4F^0$	$4d'\,^4F$
9	330.79	1.56	1.76	Cu(I)	5.07	8.82	$4p'\,^4F^0$	$4d'\,^4G$
10	410.17	1.65	1.75	In(I)	–	3.02	$5s^25p\,^2P^0$	$5s^26s\,^2S_{1/2}$
11	417.83	0.58	0.73	Ar(II)	16.64	19.61	$4s\,^4P$	$4p\,^4D^0$
12	422.26	0.57	0.85	Ar(II)	19.87	22.80	$4p\,^2P^0$	$5s\,^2P$
13	427.75	0.50	0.7	Ar(II)	18.45	21.35	$4s'\,^2D$	$4p'\,^2P^0$
14	436.20	0.32	0.95	Ar(II)	18.66	21.50	$3d^2D$	$4p'\,^2D^0$
15	451.13	3.1	3.27	In(I)	0.27	3.02	$5s^25p\,^2P^0$	$5s^26s\,^2S_{1/2}$
16	487.98	0.36	1.12	Ar(II)	17.14	19.68	$4s\,^2P$	$4p\,^2D^0$
17	501.76	0.38	0.83	Ar(II)	17.14	19.64	$4s\,^2P$	$4p\,^4D^0$
18	502.82	0.98	0.75	Cu(II)	14.43	16.87	$4d\,^3D$	$4f\,^3F^0$
19	506.063	0.72	0.8	Cu(II)	8.54	10.99	$4p\,^3P^0$	$4s^2\,^3P$
20	507.22	0.73	0.63	Cu(II)	14.42	16.87	$4d\,^3F$	$4f\,^3F^0$
21	510.00	0.40	0.52	Cu(II)	14.43	16.86	$4d\,^3D$	$4f\,^3D^0$
22	515.32	0.85	0.7	Cu(I)	3.79	6.19	$4p\,^2P^0$	$4d\,^2D$
23	520.087	0.40	0.76	Cu(I)	5.42	7.80	$4p'\,^2F^0$	$5s'\,^4D$
24	521.82	0.85	0.87	Cu(I)	3.82	6.19	$4p\,^2P^0$	$4d\,^2D$
25	522.00	0.80	0.85	Cu(I)	3.82	6.19	$4p\,^2P^0$	$4d\,^2D$
26	556.69	0.47	1.21	Se(II)				
27	557.69	0.7	0.90	In(II)	15.81	18.03	$5s7p\,^1P^0$	$5s10d\,^3D$
28	570.02	0.96	0.67	Cu(I)	1.64	3.82	$4s^2\,^2D$	$4p\,^2P^0$
29	572.18	1.41	1.15	In(II)	15.29	17.46	$5s7s\,^1S$	$5s9p\,^1P^0$
30	594.92	1.02	1.10	Ar(I)	13.28	15.35	$4p'$ [1 ½]	$6d$ [1 ½]
31	622.42	1.20	2.20	In(II)	15.77	17.76	$5s7p\,^3P^0$	$5s9d\,^3D$

equation for the electron energy distribution function (EEDF), was used. That software assumes an electric field constant in time and space. That software makes it possible to calculate the plasma EEDF by solving the Boltzmann kinetic equation in the binomial approximation for the quasistationary case.

Under the conditions of the present experiment with the duration of a voltage oscillation in the gap with a half-period of ~10 ns and a diffuse discharge, the plasma medium was in an electric field that changes more slowly than the time of establishing the electron distribution function. In this case, to find the EEDF, one can use the Boltzmann kinetic equation for the quasistationary electron distribution function.

It is known that the time to establish a quasistationary electron distribution is approximately equal to the

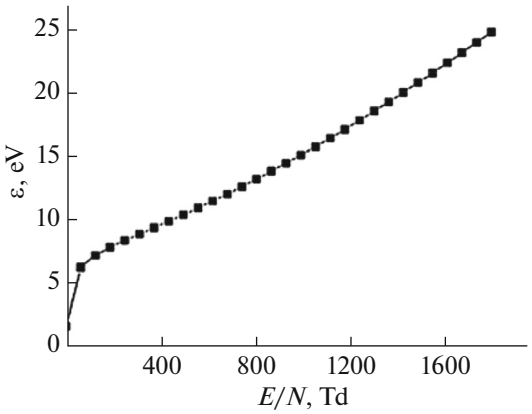

Fig. 6. Dependence of mean electron energy in plasma of the vapor-gas mixture Cu : Ar = 30 : 101000, total pressure p = 101.030 kPa and reduced electric field strength E/N.

relaxation time of the average electron energy (see equation (1) borrowed from [22]):

$$\tau = m\nu_e\varepsilon\Big/(e^2E^2), \quad (1)$$

where m is the electron mass, e is the electron charge, ε is the mean energy of electrons, E is the electric field strength, and ν_e is the frequency of elastic collisions with mixture of Ar and Cu atoms.

The estimate of τ for the present experiment gave a value of ~1×10^{-13} s, which is significantly lower than at the duration of 10 ns. Therefore, it was assumed that Bolsig + software can be used for the present experiment.

Since the effective cross sections for the electron processes for the $CuInSe_2$ molecule are not known, they were replaced by the corresponding Cu atom cross sections, since Cu is part of the chalcopyrite molecule, and the emission spectra of the chalcopyrite plasma are intense spectral lines of the atom and a single-charged copper ion Cu^+.

The parameters of the discharge plasma in a mixture of Ar with a small addition of a Cu vapor at atmospheric pressures (component ratio 101 kPa: 30 Pa and 202 kPa: 30 Pa) were determined numerically and calculated as total integrals of the EEDF. The EEDFs were found numerically by solving the Boltzmann kinetic equation in the two-term approximation via the mentioned software where the effective cross section database also includes the effective cross sections for the interaction of electrons with copper atoms. Based on the obtained EEDF, a number of plasma parameters were determined depending on the magnitude of the reduced electric field. The range of variations of the parameter E/N = 1–1800 Td (1×10^{-17}–1.8×10^{-15} V cm^2) included the values of that parameter, which were implemented in the experiment. For the vapor-gas mixture Cu : Ar = 30 : 101000 at a total pressure p_{tot} of 101.030 kPa, these E/N values were 1676 Td and 807 Td in a range of 0–100 ns and 100–480 ns, respectively, and for the gas-vapor mixture Cu : Ar = 30 : 202000 at p_{tot} of 202.030 kPa, these values of the E/N parameter were 1242 Td and 621 Td in the range 0–100 and 100–480 ns, respectively (Fig. 3). The collision integral of electrons with atoms and molecules takes into account the following processes: elastic scattering of electrons on Cu and Ar atoms, excitation of energy levels of Cu atoms (threshold energy 1.500, 3.800, 5.100 eV), ionization of Cu atoms (threshold energy 7.724 eV); excitation of the energy level of Ar atoms (threshold energy 11.50 eV), and ionization of Ar atoms (threshold energy 15.80 eV).

Figure 6 shows the dependence of the mean electron energy in the plasma of the vapor–gas mixture Cu : Ar = 30 : 101000, at a total pressure p = 101.030 kPa, on a reduced electric field strength.

The mean energy of the discharge electrons for the Cu–Ar vapor–gas mixture in the range of 30 Pa–101 kPa increased from 1.493 to 24.72 eV, and for the Cu–Ar mixture in the range of 30 Pa–202 kPa, it also increased from 1.641 to 24.73 eV, since the reduced electric field strength increased from 1 to 1800 Td (Fig. 6). In this case, a regularity of the increased rate of its change in the range of 1–63 Td was observed.

In Table 2, the results of calculating the transport characteristics of electrons are presented: ε eV—mean energies; T_e K—temperature, and V_{dr}—drift velocity of electrons for two mixtures of Cu vapor with Ar.

The electron drift velocity was 9.0×10^5 m/s for the plasma field strength of 4×10^7 and 1.0×10^6 m/s for the plasma field strength of 2×10^7 V/m, which is reached after 100 ns from the start of the breakdown in the interelectrode gap (the amplitude of the voltage pulses decreases to 20000 V, Fig. 3) for the mixture: Cu–Ar = 30 Pa–101 kPa; and for the Cu–Ar mixture = 30 Pa–202 kPa, 7.0×10^5 and 1.1×10^6 m/s, respectively.

The electron concentration is 5.3×10^{19}–3.8×10^{19} m^{-3} at a current density (7.65–6.12) $\times 10^6$ A/m^2 on the surface of the electrode of the radiation source 0.196×10^{-6} m^2 for a reduced electric field strength E/N = 1676 Td which existed in the discharge gap for the first 100 ns, and for a reduced electric field strength E/N = 807 Td which existed in the discharge gap after 100 ns for the Cu–Ar = 30 Pa–101 kPa mixture. For the second mixture Cu–Ar = 30 Pa–202 kPa, the electron concentration was 8.2×10^{19}–3.5×10^{19} m^{-3} at a current density (9.2–6.1) $\times 10^6$ A/m^2 on the surface of the electrode of the radiation source (0.196×10^{-6} m^2) for the reduced intensity the electric field E/N = 1242 Td, which existed in the discharge gap for the first 100 ns and for a reduced electric field strength E/N = 621 Td, which existed in the discharge gap after 100 ns.

Figure 7 shows the dependence of specific power losses η of the discharge on the process of electron collisions with copper and argon atoms vs the parameter

Table 2. Transport characteristics of electrons for 0–100 ns with electric field strength $E = 4 \times 10^7$ V/m for a mixture: Cu–Ar = 30 Pa–101 kPa, with electric field strength $E = 6 \times 10^7$ V/m for a mixture: Cu–Ar = 30 Pa–202 kPa

E/N, Td	Mixture: Cu–Ar = 30 Pa–101 kPa			E/N, Td	Mixture: Cu–Ar = 30 Pa–202 kPa		
	ε, eV	T_e, K	V_{dr}, m/s		ε, eV	T_e, K	V_{dr}, m/s
63	6.169	71560.4	1.5×10^6	63	6.223	72186.8	1.1×10^6
807	13.11	152076	1.0×10^6	621	11.39	132124	1.1×10^6
1676	23.09	267844	9.0×10^5	1242	17.77	206132	7.0×10^5
1800	24.72	286752	8.9×10^5	1800	24.73	286868	6.6×10^5

E/N in plasma for Cu : Ar = 30 : 101000 Pa at a p_{tot} = 101.030 kPa.

Specific losses of discharge power in the processes of elastic electron scattering by copper and argon atoms are presented in equation (2):

$$\eta_R = (1/W)(2m/M_R)(N_R/N) \times (2/m)^{\frac{1}{2}} \int_0^\infty U^2 Q_R(U)[f(U) + kT(df(U)/dU]dU. \quad (2)$$

Specific losses of discharge power in the processes of excitation and ionization of Cu and Ar atoms are presented in Equation 4:

$$\eta_{Rj} = (1/W)(N_{Rj}/N)U_{Rj} \times (2/m)^{\frac{1}{2}} \int_{u_{Rj}}^\infty Uf(U)Q_{Rj}(U)dU. \quad (3)$$

In equations (2) and (3) above: T is the gas temperature; k is the Boltzmann constant; e and m are the charge and the mass of an electron, respectively; M_R is the mass of the Cu or Ar atom; $\varepsilon = e \times U$ is the electron energy; N_R is the concentration of neutral unexcited Cu or Ar atoms, N_{Rj} is the concentration of Cu or Ar atoms participating in the jth excitation process, N is the total concentration of a mixture of neutral unexcited particles, $Q_R(U)$ is the effective cross section for the elastic scattering of electrons by copper or argon atoms, $Q_{Rj}(U)$ is the effective cross section for the jth inelastic process in Cu or Ar atoms, in which the electron loses energy, U_{Rj} is the energy of this process, W is the total discharge power given by the condition

$$\eta_R + \sum_j (\eta_{Rj_{sj}}) = 1,$$

$f(U)$ is the isotropic part of the EEDF, normalized by the condition:

$$\int_0^\infty U^{1/2} f(U)dU = 1.$$

The specific losses of discharge power in a mixture of Cu vapor with Argon (Cu–Ar 30 Pa–101 kPa) due to inelastic collisions of electrons with the mixture components for a reduced electric field strength of 1667 Td are maximum for ionization of Ar atoms (Fig. 7); for their excitation of the energy state with a threshold energy of 11.5 eV, they reach 34 and 16%, respectively. For the second mixture (Ar–Cu = 202 kPa–30 Pa), they reach 37 and 21% at a reduced electric field strength of 1242 Td.

For a reduced field strength E/N = 807 Td, which occurred after 100 ns since the breakdown of the interelectrode gap in the first mixture, they did not exceed 39 and 28%, respectively, and for the second mixture—after 100 ns, for E/N = 621 Td, 39 and 33%, respectively.

For copper atoms, they did not exceed 0.07% (for excitation of the resonance state $^2P_{3/2,1/2}$) for the first mixture at E/N = 1667 Td, and for the second one—0.06% at E/N = 1242 Td.

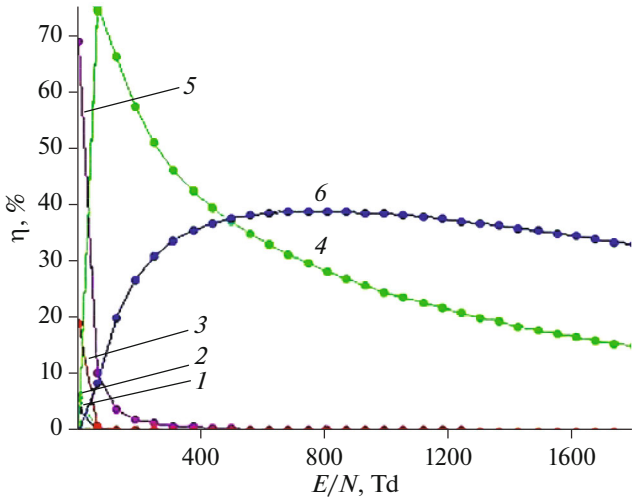

Fig. 7. Dependence of specific losses of discharge power on processes of collisions of electrons with Cu and Ar atoms on the E/N parameter in plasma for a Cu : Ar = 30 : 101000 mixture at a total pressure of P = 101.030 kPa: (*1*) excitation of the state of a Cu atom (threshold energy 1.5 eV); (*2*) excitation of the state of a Cu atom (threshold energy 1.5 eV); (*3*) elastic scattering by Ar atoms; (*4*) excitations of energy level of Ar atoms (threshold energy 11.5 eV); (*5*) excitation of resonance state $^2P_{3/2,1/2}$ of a Cu atom (threshold energy 3.8 eV); and (*6*) ionization of Ar atoms (threshold energy 15.8 eV).

Table 3. Values of collision rate constants of electrons with Cu and Ar atoms $k1$–$k5$ for the electric field strength $E = 4 \times 10^7$ V/m) for the mixture: Cu–Ar = 30 Pa–101 kPa and for the electric field strength $E = 6 \times 10^7$ V/m) for the mixture: Cu–Ar = 30 Pa–202 kPa

Mixture Cu : Ar = 30Pa : 101 kPa; total pressure 101030 Pa					
No.	Process	k, m^3/s	E/N = 1676 Td	E/N = 807 Td	E/N = 63 Td
1	Cu elastic	$k1$	0.1178E-11	0.1147E-11	0.8481E-12
2	Ar effective (momentum)	$k2$	0.2549E-12	0.2243E-12	0.1363E-12
3	Cu excitation threshold energy 3.80 eV	$k3$	0.9495E-12	0.7831E-12	0.3389E-12
4	Ar excitation threshold energy 11.50 eV	$k4$	0.2134E-13	0.9747E-14	0.2417E-15
5	Ar ionization potential energy 15.80 eV	$k5$	0.3285E-13	0.9783E-14	0.2001E-16
Mixture Cu : Ar = 30 Pa–202 kPa; total pressure 202030 Pa					
No.	Process	k, m^3/s	E/N = 1242 Td	E/N = 621 Td	E/N = 63 Td
1	Cu elastic	$k1$	0.1174E-11	0.1124E-11	0.8552E-12
2	Ar effective (momentum)	$k2$	0.2426E-12	0.2137E-12	0.1379E-12
3	Cu excitation threshold energy 3.80 eV	$k3$	0.8916E-12	0.7184E-12	0.3451E-12
4	Ar excitation threshold energy 11.50 eV	$k4$	0.1602E-13	0.6984E-14	0.2546E-15
5	Ar ionization potential energy 15.80 eV	$k5$	0.2076E-13	0.5967E-14	0.2140E-16

The maximum specific loss of discharge power in the first mixture is observed to excite the energy level of Ar atoms with a threshold energy of 11.5 eV and reach a value of 76% for a reduced electric field strength of 63 Td and 70% for excitation of a resonant state of $^2P_{3/2,1/2}$ Cu atoms for a reduced electric field strength fields of 1 Td, and for the second mixture, 80% for excitation of the energy level of Ar atoms with a threshold energy of 11.5 eV for excitation of the energy level of Ar atoms with a threshold energy of 11.5 eV for E/N = 63 Td and 61% for excitation of resonance state $^2P_{3/2,1/2}$ Cu atoms for E/N = 1 Td. With an increase in the E/N parameter to 1800 Td, the specific loss of discharge power in mixtures reached 33% for the ionization of Ar atoms by electrons.

The rate of the rise and fall of discharge power losses on the processes of excitation of electronic states, as well as ionization and its magnitude (Fig. 7) are related to the nature of the dependence of the effective cross sections of inelastic collisions of electrons with mixture components on electron energies, their absolute values, and with the dependence of the electron distribution function on the magnitude of a reduced field strength and the threshold energy of the process. The losses in the discharge power due to the excitation and ionization of Cu atoms in the range of a reduced electric field strength at which the used here plasma source operated (1676–807 Td and 1242–621 Td) were small, due to a low content of a Cu vapor in the mixture.

Table 3 shows the highest values of the rate constants $k1$–$k5$ of the collisions of electrons with Cu and Ar atoms for the reduced electric field strength, which are a measure of the efficiency of the process for the mixture Cu : Ar = 30 Pa : 101 kPa, the total pressure being 101030 Pa, and for the mixture Cu : Ar = 30 Pa–202 kPa, p_{tot} being 202030 Pa. They vary in the range 0.2140×10^{-16}–0.1178×10^{-11} m^3/s for characteristic values of the reduced electric field strength. The rate constant of elastic scattering of electrons by Cu atoms is maximum and with decreasing values of a reduced electric field strength decreases almost 1.4 times for both mixtures. The excitation rate constant of the resonance state of Cu for the first mixture is higher, with the values of 0.9495×10^{-12} m^3/s and 0.7831×10^{-12} m^3/s for a reduced electric field strength at which the plasma source of film deposition operates: E/N = 1676 Td and E/N = 807 Td.

Transmission Spectra of Radiation by Chalcopyrite Films

Detailed results of the study of the absorption coefficient of radiation for films based on the $CuInSe_2$ compound as a function of wavelength are given in [1, 23]. Thus, in the 200–300 nm wavelength range, the absorption coefficient decreased from 6×10^5 to 4×10^5 cm^{-1}, and in the range of 300–400 nm, the absorption coefficient was approximately constant and was equal to 4×10^5 cm^{-1}. With an increase in the wavelength from 400 to 1000 nm, it decreased to 10^4 cm^{-1}, and in the range of 1000–1200 nm, the absorption coefficient decreased exponentially to 10 cm^{-1}. As can be seen from these data, the absorption coefficient of chalcopyrite films is large and strongly depends on the wavelength of the incident radiation.

Let us consider the relative transmission spectra of thin films synthesized from the products of destruction of chalcopyrite electrodes of an overstressed nanosecond discharge in argon and air. The characteristic transmission spectra of radiation in the spectral region 200–500 nm of the synthesized chalcopyrite films at different argon pressures and atmospheric air pressure are shown in Fig. 8. The transmission of chalcopyrite films, as compared with that of the substrate, decreased by approximately 2–3 times and was minimal for mixtures based on argon at p (Ar) = 101 kPa. The shape of the transmission spectra of chalcopyrite films at argon pressures of 13.3 and 101 kPa was the same.

The minimum transmission of chalcopyrite films, which was about an order of magnitude smaller than the transmission of a clean substrate, was obtained for samples synthesized in air at atmospheric pressure. The presence of oxygen in such a plasma can lead to the implantation it into the film, which can adversely affect its photovoltaic characteristics. If, in this case, the coefficients of the conversion of radiation energy into electrical energy are sufficiently large, this opens up prospects for creating an open plasma-chemical reactor based on atmospheric air, in which deposition of chalcopyrite films of a large area is possible. An additional advantage of such a reactor will be the complete absence of vacuum technology and the use of the maximum available gas medium. The technology based on the use of atmospheric or pressurized argon is also promising and can be implemented in the gas flow mode without the use of vacuum technology.

Strong absorption of radiation from a deuterium lamp by chalcopyrite films in a wavelength range 200–500 nm is due to the fact that when sputtering chalcopyrite films by the gas-discharge method using massive chalcopyrite electrodes, they repeat the stoichometry of the electrodes. But for the accurate determination of the composition of the synthesized chalcopyrite films, it is necessary to carry out a study of their composition by both X-ray diffraction and electron spectroscopy.

Whith replacing a deuterium lamp with a thermal one, the transmission spectra of the same chalcopyrite films were investigated in a spectral range of 400–800 nm. But even in this case, the main features of the transmission spectra of chalcopyrite films at different argon pressures and air pressures remained unchanged.

Comparison of the transmission spectra with regard to the probing radiation spectra and the transmission spectrum of the substrate with the dependence of the absorption coefficient on the wavelength are qualitatively correlated with each other, which indicates that the composition of the films is close to the composition of the electrodes.

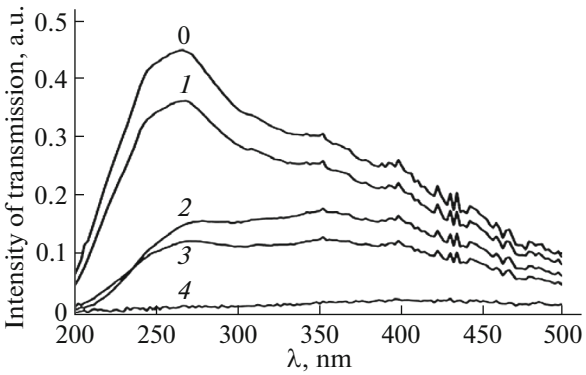

Fig. 8. Transmission spectra of samples of chalcopyrite films deposited on quartz substrates depending on pressure and type of gaseous medium: (0) without sample; (*1*) pure quartz glass; (*2*) electrodes with $CuInSe_2$ at $p(Ar)$ = 13.3 kPa; (*3*) electrodes with $CuInSe_2$ at $p(Ar)$ = 101 kPa; and (*4*) electrodes with $CuInSe_2$ at $p(air)$ = 101 kPa.

CONCLUSIONS

Thus, it was demonstrated that at argon pressures of 101 and 202 kPa between the chalcopyrite electrodes with a distance between them of 0.1 cm, a sufficiently uniform nanosecond discharge is ignited with a pulsed electrical power of 5–11 MW and a plasma energy input per pulse of 0.40; 0.44 J.

Spectroscopic diagnostics of chalcopyrite plasma showed that the spectral lines of Cur atoms in a range of 200–230 nm and the spectral lines of In atoms, copper Cu^+ and indium In^+ ions in a longer wavelength region are the most intense in the emission spectra. At the same time, with an increase in the argon pressure from 101 to 202 kPa, the intensities of the Cu atom lines in a spectral range 200–230 nm, and the intensities of the ion lines in a spectral range of 230–460 nm also increased. The nature of the emission spectrum presumes the existence of selective mechanisms for the formation of excited atoms and ions of Cu and In in plasma, associated with the transfer of energy from metastable atoms and molecules of argon. Based on the measured relative intensities of the spectral lines of atoms and Cu and In ions, it is possible to make estimates of the temperature and density of electrons in the plasma under study. The following most intense lines from a spectral range of 300–460 nm can be used to diagnose the deposition of chalcopyrite films in real time: 307.38 nm Cu(I), 329.05 nm Cu(I), 410.17 nm In(I), and 451.13 nm In(I).

The mean electron energy increased from 1.493 to 24.72 eV with a change in the E/N parameter from 1 to 1800 Td in plasma on a mixture with Ar pressure equal to 101 kPa. The temperature of the electrons was 71560.4, 152076, and 267844 K with the parameter values E/N = 63, 807, and 1676 Td, respectively. The electron concentration was in a range of 5.3×10^{19}–3.8×10^{19} m^{-3} at a current density of (7.65–6.12) ×

10^6 A/m^2 on the electrode surface at a parameter value of $E/N = 1676$ Td, which is realized in the discharge in the first 100 ns and for the reduced electric field strength $E/N = 807$ Td, which existed in the discharge gap after 100 ns.

The specific losses of the discharge power in the mixture Cu : Ar = 30 Pa : 101 kPa for inelastic collisions of electrons with mixture components were the greatest for Ar atoms and reached 76% (excitation of the energy level with a threshold energy of 11.5 eV) for the parameter E/N = 63 Td and 80% for the same value of the reduced electric field strength for the vapor-gas mixture Cu : Ar = 30 Pa : 101 kPa; for Cu atoms they had a maximum value of 70% to excite the resonance state $^2P_{3/2,1/2}$ in the mixture Cu : Ar = 30 Pa : 101 kPa for reduced electric field intensity 1 Td.

The rate constants of electronic processes varied in a range of 0.2140×10^{-16}–0.1178×10^{-11} m^3/s. The excitation rate constant of the resonance level of the Cu atom in the first mixture of Cu vapor with Ar was 0.9495×10^{-12} and 0.7831×10^{-12} m^3/s for the experimental value of the reduced electric field strength $E/N = 1676$ Td and $E/N = 807$ Td, while for the second mixture (Ar = 202 kPa) it had a lower value—0.8916×10^{-12} and 0.7184×10^{-12} m^3/s for E/N = 1242 Td and $E/N = 621$ Td.

The study of the relative transmission spectra of probe radiation in the 200–800 nm wavelength range with chalcopyrite films synthesized by the pulsed gas-discharge method showed that the least transmission is characteristic for films synthesized at atmospheric pressures of argon and air.

CONFLICT OF INTEREST

The authors declare to have no conflict of interest.

REFERENCES

1. Novikov, G.F. and Gapanovich, M.V., *Phys.-Usp.*, 2017, vol. 60, no. 2, pp. 161–178.
2. Shuaibov, A.K., Minya, A.Y., Chuchman, M.P., Malinina, A.A, et al., *Plasma Res. Express*, 2018, vol. 1, art. ID 015003.
3. Mesyats, G.A., *Phys.-Usp.*, 1995, vol. 38, no. 6, pp. 567–590.
4. Shuaibov, O.K., Malinina, A.O., Malinin, O.M., *New Gas-Discharge Methods for Obtaining Selective Ultraviolet and Visible Radiation and the Synthesis of Nanostructures of Transition Metal Oxides*, Uzhhorod: Hoverla, 2019.
5. Danilyuk, P.S., Popovich, K.P., Puga, P.P., Gomonai, A.I., et al., *Opt. Spectrosc.*, 2014, vol. 117, no. 5, pp. 759–763.
6. Holovey, V.M., Popovych, K.P., Prymak, M.V., Birov, M.M., et al., *Phys. B* (Amsterdam), 2014, vol. 450, pp. 34–38.
7. Kozyrev, A.V., Kozhevnikov, V.Yu., Kostyrya, I.D., Tarasenko, V.F., et al., *Atmospheric and Oceanic Optics*, 2011, vol. 24, no. 11, pp. 1009–1017.
8. Rybka, D.V., Burachenko, A.G., Kozhevnikov, V.Yu., Kozyrev, A.V., et al., *Atmospheric and Oceanic Optics*, 2014, vol. 27, no. 4, pp. 311–315.
9. Lomaev, M.I., Beloplotov, D.V., Sorokin, D.A., Tarasenko, V.F., *Opt. Spectrosc.*, 2016, vol. 120, no. 2, pp. 171–175.
10. Beloplotov, D.V., Trigub, M.V., Tarasenko, V.F., Evtushenko, G.S., et al. *Atmospheric and Oceanic Optics*, 2016, vol. 29, no. 4, pp. 371–375.
11. Shuaibov, A.K., Laslov, G.E., Kozak, Ya.Yu. *Opt. Spectrosc.*, 2014, vol. 116, no. 4, pp. 552–556.
12. Shuaibov, A.K., Minya, A.Y., Malinina, A.A., Malinin, A.N., et al. *Am. J. Mechan. Mater. Eng.*, 2018, vol. 2, no. 1 pp. 8–14.
13. Shuaibov, A.K., Minya, A.Y., Gomoki, Z.T., Danilo, V.V., et al. *Elektronnaya Obrabotka Materialov*. 2018, vol. 54, no. 1 pp. 46–50. (in Russian).
14. Ampilov, A.M., Barkhudarov, E.M., Kozlov, Yu.N., Kossyi, I.A., et all. *Plasma Phys. Rep.*, 2019, vol. 45, no. 3, pp. 268–273.
15. Ivanov, I.G., *Avtometriya*, 1984, vol. 1, pp. 19–34.
16. Pashchina, A.S., Efimov, A.V., Chinnov, V.F., *High Temp.*, 2017, vol. 55, no. 5, pp. 650–664.
17. Baksht, E.Kh., Burachenko, A.G., Lomaev, M.I., Panchenko, A.N., et al., *Quantum Electron.*, 2015, vol. 45, pp. 366–370.
18. Trenkin, A.A., Karelin, V.I., Shibitov, Yu.M., Blinova, O.M., et al. *Techn. Phys.*, 2017, vol. 62, no. 9, pp. 1419–1423.
19. Tarasenko, V. F, Yakovlenko, S. I., *Phys. Usp.*, 2004, vol. 47, pp. 887–905.
20. Tarasenko, V.F., *Runaway electrons preionized diffuse discharge*. New York: Nova Science Publishers, 2014.
21. Kozhevnikov, V.Yu., Kozyrev, A.V., Dmitrieva, N. M., *Russ. Phys. J.*, 2014, vol. 57, no. 3/2, pp. 130–133.
22. Mkrtchyan, M.M. and Platonenko,Viktor T. *Soviet Journal of Quantum Electronics*, 1979, 9, no. 8, pp. 967–971.
23. Vertsimakha, Ya., Lutsuk, P., Lytvyn, O., Gashin, P., *Ukr. J. Phys.* 2007, vol. 52 no. 4, pp. 399–405.